

Probing hydrogenated amorphous silicon surface states by spectroscopic and real-time second-harmonic generation

I. M. P. Aarts, J. J. H. Gielis, M. C. M. van de Sanden, and W. M. M. Kessels*

Department of Applied Physics, Eindhoven University of Technology, P.O. Box 513, 5600 MB Eindhoven, The Netherlands

(Received 12 April 2005; revised manuscript received 28 October 2005; published 26 January 2006)

The second harmonic generation (SHG) signal from hydrogenated amorphous silicon (*a*-Si:H) thin films is measured *in situ* and in real-time during film growth. Polarization and spectral dependences of the SHG radiation are investigated for as-deposited films and after subsequent molecular oxygen dosing in order to confirm the sensitivity of SHG to *a*-Si:H surface states. On the basis of these experiments, we conclude the SHG radiation is partly generated at the surface (*a*-Si:H/vacuum interface) and the microscopic origin of the SHG signal appears to be dangling and surface Si-Si bonds. This has been supported by simulations of the nonlinear surface response for the different polarization configurations using an excitonic line shape model with two resonances. Furthermore, real-time measurements during film growth, up to a film thickness of 412 nm, demonstrate the potential of the technique to monitor surface states during the deposition process of *a*-Si:H films.

DOI: [10.1103/PhysRevB.73.045327](https://doi.org/10.1103/PhysRevB.73.045327)

PACS number(s): 73.20.At, 42.65.Ky

I. INTRODUCTION

During thin film growth of amorphous semiconductor and dielectric materials, coordination defects and weak bonds at the surface play a crucial role in the adsorption process of growth precursors. For example, for hydrogenated amorphous silicon (*a*-Si:H), a material used in solar cells, displays, and imaging devices and generally synthesized by plasma or thermal decomposition of silane, surface processes have been proposed that involve (i) the adsorption of radicals on undercoordinated Si atoms (dangling bonds);¹⁻³ (ii) the adsorption of radicals near overcoordinated Si atoms (floating bonds) in which these coordination defects are healed;⁴ and (iii) direct insertion of radicals into surface Si-Si bonds such as strained Si-Si bonds.⁵ Also from a device perspective, coordination defects and weak bonds at surfaces are pivotal as the performance of most semiconductor devices is ruled by interface properties. Examples are the channel region next to the gate material in thin film transistors and heterojunctions in thin film solar cells. Within the current trend of miniaturization of device dimensions, surface and interface dangling bonds, floating bonds and weak bonds will only become more important.

Despite the importance of surface coordination defects, diagnostic techniques for probing these surface states are not readily available. Preferentially, such techniques should be applicable *in situ* and in real-time during processing as it is essential to obtain a fundamental understanding of the role of these surface states during the growth process of the materials and their appearance during device formation.⁶⁻⁸ In this paper, we apply the nonlinear optical technique of second harmonic generation (SHG), which has an intrinsic interface sensitivity and appears to be a promising technique to detect surface states of *a*-Si:H.⁹

The potential of SHG can best be illustrated by the numerous surface science studies on crystalline silicon (*c*-Si). For *c*-Si, the surface selectivity of SHG arises because the bulk inversion symmetry forbids an electric dipole contribu-

tion, while the broken symmetry at the surface or interface allows a dipole contribution. Furthermore, SHG is resonantly enhanced when choosing the fundamental or the second harmonic photon energy to coincide with electronic surface state transitions.¹⁰ As a result, surface states for Si(100) and Si(111) have been probed by SHG.¹¹⁻¹⁶ For example, from spectroscopic SHG surface Si dangling bonds have been identified for photon energies in the range of ~ 1.0 to ~ 1.5 eV,¹¹⁻¹³ while Suzuki was able to resolve that surface Si dangling bonds are probed by a two-photon transition around 1.2 eV and a one-photon transition around 1.4 eV for the Si(111)-(7 \times 7) surface.¹⁴ Furthermore, Si-Si bonds in a strained surface layer have been observed by a two-photon resonance at ~ 3.3 eV.¹¹⁻¹⁶

When comparing with *c*-Si, *a*-Si:H lacks the long-range order which results in a broad dielectric function with a maximum close to the critical point transitions E'_0/E_1 as observed for *c*-Si.¹⁷ Likewise, the density of states distribution is also broadened compared to *c*-Si forming band tails and localized states in the gap. The band tails, which are attributed to strained Si-Si bonds or weak bonds in the amorphous matrix, lead to an exponentially increasing absorption with increasing photon energy within the range ~ 1.4 – 1.9 eV, i.e., the Urbach tail. Undercoordinated defects or dangling bonds form localized states, which lie in the band gap (Ref. 18, and references therein). These defects, in the bulk ($\sim 10^{16}$ cm⁻³) and in the surface region of *a*-Si:H ($< 10^{12}$ cm⁻²), are generally probed by subgap absorption spectroscopy techniques, such as photothermal deflection spectroscopy¹⁹ and, more recently, also with cavity ring-down spectroscopy.²⁰ Naturally amorphous materials possess bulk inversion symmetry, which excludes second harmonic dipole contributions from the bulk.

Considering these properties of *a*-Si:H, it is tempting to investigate whether SHG can reveal information about the surface states of *a*-Si:H. This research question has not been addressed yet in the literature by other research groups, although some *ex situ* SHG data have been reported. Erley and

Daum showed, for comparison purposes only, the SHG spectrum of an a -Si:D film for a fundamental photon energy range of 1.2–2.5 eV. They observed only a very weak, featureless SHG signal which was an order of magnitude less than the SHG radiation from the c -Si.²¹ Furthermore, Alexandrova *et al.* measured the SHG radiation from a 125 nm thick a -Si:H film but only at a single photon energy of 1.17 eV.^{22,23} We have recently reported a more extensive *ex situ* investigation on a -Si:H films of 9 and 1031 nm thickness, including the azimuthal and polarization dependence, and a spectroscopic scan from 1.0–1.7 eV.⁹ Isotropic and resonant signals were observed, however, the a -Si:H under investigation was native-oxide covered and also no direct evidence for probing surface states could be obtained from these experiments.

In this paper, we report on an *in situ* SHG study on as-deposited a -Si:H films prepared by hot-wire chemical vapor deposition (HW-CVD). The polarization and spectral dependence of the SHG radiation is investigated for fundamental photon energies ranging from 1.0 to 1.7 eV, while oxygen dosing experiments are carried out to prove surface sensitivity. On basis of c -Si studies reported in the literature, the microscopic origin of the SHG from a -Si:H thin films will be discussed. Moreover, the first results on real-time monitoring of a -Si:H film growth and sequential surface oxidation by SHG will be reported.

II. EXPERIMENTAL DETAILS

The a -Si:H films were deposited in a high-vacuum chamber (base pressure $<10^{-9}$ Torr) by HW-CVD. A tungsten filament was heated to 2050 ± 200 °C in silane gas (SiH_4 , purity $>99.995\%$) at a pressure of 10^{-4} Torr. The films were deposited on fused silica substrates located at 6.8 cm from the filament and heated up to 450 °C by a radiative heater from the back of the substrate. The temperature was actively controlled using thermocouples glued on the substrate. The deposition rate (1.3 nm/min) and dielectric functions of the a -Si:H films were deduced by real-time spectroscopic ellipsometry using photon energies between 0.7 and 5.0 eV. These experiments were carried out on c -Si substrates in a separate experiment. Surface oxidation of the a -Si:H films was performed by exposing the as-deposited films to molecular oxygen (O_2 , purity 99.999%) by backfilling the chamber to an O_2 pressure of 7.5×10^{-5} Torr through a leak valve.

The SHG experiments were carried out over a photon energy range of 1.0 to 1.7 eV using the tunable idler beam of an optical parametric oscillator (OPO) pumped by a frequency-tripled Q -switched neodymium yttrium aluminium garnet (Nd:YAG) laser with a 6 ns pulse duration and 30 Hz repetition rate (Spectra-Physics MOPO-710 and GCR-230). The wavelength of the laser radiation was checked independently by a calibrated monochromator leading to an accuracy in fundamental photon energy of ± 0.003 eV. The fundamental radiation energy was set by a combination of a half-wave retardation plate and a Glan-Thompson polarizer such that the laser fluence on the sample was constant at 60 mJ/cm² per pulse, which is below the

threshold for crystallization of the a -Si:H and no influence of the laser on the a -Si:H films was observed. The polarization of the fundamental and SHG radiation were controlled by a half-wave retardation plate and a Glan-Thompson polarizer, respectively. The laser beam was incident on the sample at 35° with respect to the surface normal. An absorptive filter was used to block SHG radiation present in the fundamental beam before the beam entered the vacuum chamber while the reflected fundamental radiation from the substrate was suppressed against the SHG radiation using an absorptive filter and a monochromator. Photon counting was applied using a photomultiplier tube and gated electronics. The stability of the laser system was monitored using the SHG radiation produced by a GaAs(100) sample in a reference channel. The SHG spectra were corrected for the linear transmission of the detection system that was measured using a calibrated ribbon lamp. A very low transmission of the monochromator for P -polarized light around 2.6 eV was observed,²⁴ causing a relatively large uncertainty in the detected SHG signal for a fundamental photon energy of ~ 1.3 eV. This uncertainty is indicated in the SHG spectra by error bars. Furthermore, the fused silica substrates and vacuum windows did not produce a detectable level of SHG radiation.

III. RESULTS AND DISCUSSION

First, we will consider the SHG radiation of a 9 nm thick as-deposited a -Si:H film. For this film, measurements were carried out as a function of the polarization angle of the fundamental radiation with a fixed output polarization, and as a function of the photon energy for the polarization configurations: (p, P) which stands for p -input and P -output polarizations; (s, P) s -input and P -output polarization; and (mix, S) 45° input and S -output polarizations. The results are given in Figs. 1 and 2.

The polarization dependence in Fig. 1 for a photon energy of 1.2 eV reveals a clear periodic variation for the output P signal, while the output S signal shows some variation, though it hardly exceeds the noise level. This polarization dependence can be well fitted by the expressions¹⁰

$$I_P(2\omega) = a \sin^4(\phi) + b \sin^2(\phi)\cos^2(\phi) + c \cos^4(\phi),$$

$$I_S(2\omega) = d \sin^2(\phi)\cos^2(\phi) \quad (1)$$

that describe the output P and S polarization, I_P and I_S , respectively, for a nonchiral isotropic surface, which is the expected symmetry for an amorphous film. The parameters a – d are related to the appropriate combination of Fresnel coefficients, and amplitudes and complex phases of the second-order nonlinear susceptibility tensor elements $\chi_{zzz}^{(2)}$, $\chi_{xxx}^{(2)} = \chi_{yzy}^{(2)}$, $\chi_{zxx}^{(2)} = \chi_{zyy}^{(2)}$, that describe ∞m -symmetry.¹⁰ The polarization angle ϕ is defined as the angle between the polarization vector of the incident fundamental beam and the plane of incidence (p at $\phi=0$ and 180 degrees; s at $\phi=90$ and 270 degrees). The SHG spectra in Fig. 2 show a dependence on the photon energy with the largest SHG signal observed for the (p, P) polarization configuration and almost no signal for

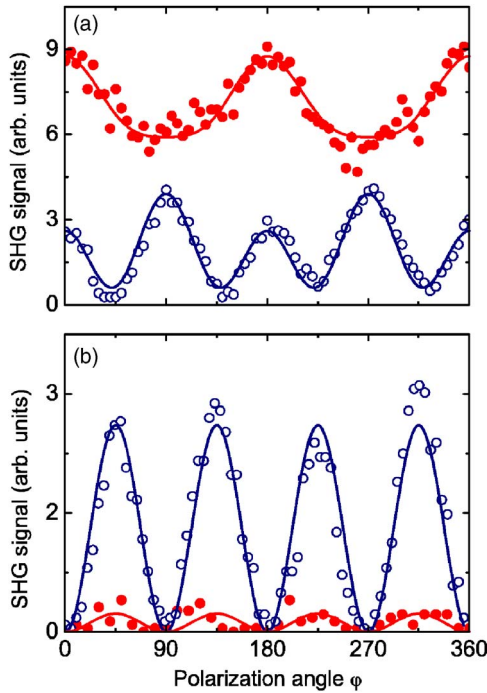


FIG. 1. (Color online) The SHG signal from a 9 nm thick a -Si:H film as a function of the polarization angle of the incident fundamental beam, measured with respect to the plane of incidence (p polarization corresponds to $\varphi=0^\circ$ and 180° , and s polarization to $\varphi=90^\circ$ and 270°). (a) P -output SHG radiation and (b) S -output SHG radiation both showing the as-deposited films (closed symbols) and films exposed to O_2 (open symbols). The photon energy of the fundamental beam is 1.2 eV. Solid lines are fits to Eq. (1).

(mix, S), which is in agreement with Fig. 1. The overall trend of the spectral dependence was confirmed by a good reproducibility throughout the measurements: a higher signal for photon energies above 1.3 eV (with a maximum around ~ 1.6 eV) as well as an apparent feature between 1.0 and 1.3 eV.

Insight into whether a SHG signal is generated at the surface of the film can be obtained by modifying the surface properties, for example, by dosing with O_2 which is known to quench certain surface states of silicon.^{14,15,25} In general, a -Si:H films are found to be relatively more resistant against surface oxidation than c -Si surfaces, which can be attributed to the almost completely H-passivated surface.²⁶ Figures 1 and 2 show the results obtained after O_2 dosing of the film with a total exposure of 2.3×10^4 L. Large changes in the SHG signal were observed by the O_2 dosing as is especially clear from the polarization dependence in Fig. 1. The P -output polarization collapsed drastically for p -input polarization. On the other hand, the S -output polarization increased considerably for the mix -input polarization. The polarization dependence of the O_2 dosed a -Si:H film could be fitted well by the expressions of Eq. (1). The isotropic nature of the SHG signal was further confirmed by the fact that no azimuthal dependence of the signal was observed for this film in an *ex situ* experiment. These results on O_2 dosed HW-CVD a -Si:H films are, therefore, in agreement with previous *ex situ* SHG results on native-oxide covered

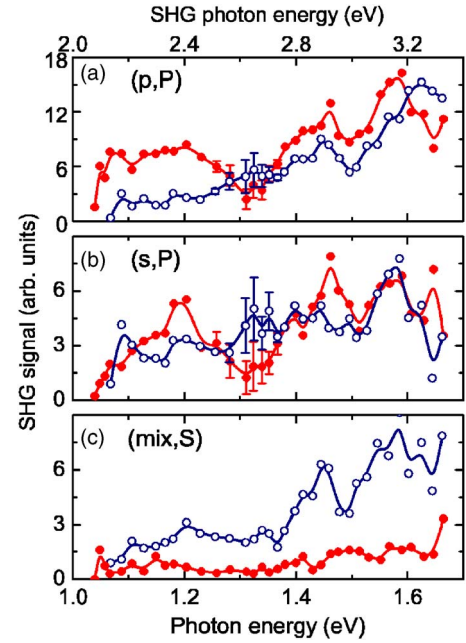


FIG. 2. (Color online) SHG spectra for three polarization combinations (a) (p, P), (b) (s, P), and (c) (mix, S) as a function of the fundamental photon energy for the as-deposited 9 nm thick a -Si:H film (closed symbols) and for the film after exposure to 2.3×10^4 L of O_2 (open symbols). In (a) and (b), the error bars around a fundamental photon energy of 1.3 eV denote the uncertainty associated with a correction for the optical transmission of the detection system. The solid lines are B splines to the data.

(a -Si:H) films deposited by plasma-enhanced⁹ CVD. Significant changes in the SHG signal are also observed in the spectral data: a decrease for (p, P) especially in the region below 1.3 eV, while there is also a smaller decrease for (s, P) (in agreement with Fig. 1). For (mix, S), an increase is observed for the whole photon energy range, while being most pronounced for the region above 1.3 eV. In this energy range, (p, P) shows a slight decrease in SHG signal, while no clear change is apparent for (s, P).

These observations prove there is a contribution from the surface to the SHG signal, however, it is not straightforward to determine its “microscopic” origin due to several reasons. First of all, for this thin a -Si:H film, also SHG generated at the buried interface can contribute to the total detected SHG signal. This contribution can be eliminated by going to thick films when the a -Si:H becomes opaque for the visible SHG radiation generated at the interface, as we will discuss in detail below. However, for such thick films, interference effects at the pump wavelength complicate the interpretation of the spectral data. Furthermore, the SHG radiation might also have nonlocal bulk¹⁰ and electric-field-induced contributions.²⁷ Also, the interpretation for (p, P) is complicated because three independent second-order nonlinear tensor elements ($\chi_{zzz}^{(2)}$, $\chi_{xzx}^{(2)}$, and $\chi_{zxx}^{(2)}$) are probed simultaneously. On the other hand, for (s, P) and (mix, S), only one tensor element is probed ($\chi_{zyy}^{(2)}$ and $\chi_{yzy}^{(2)}$, respectively), but even for these polarization configurations, the interpretation can be complicated as different microscopic contributions to the

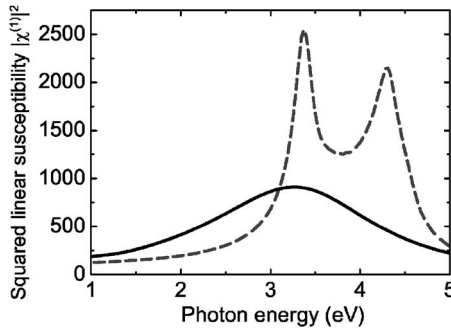


FIG. 3. The squared linear bulk susceptibility $|\chi^{(1)}|^2$ of *c*-Si (dashed line) and *a*-Si:H (solid line) as determined from the dielectric function of the materials measured by spectroscopic ellipsometry. The data for the *c*-Si have been obtained at room temperature, the data for *a*-Si:H at a substrate temperature of 450 °C.

SHG radiation might spectrally overlap and interfere. For example, the Si(111)-(7×7) surface destructive interference has been observed for the SHG signal generated by the dangling bonds and the strain-induced resonance.^{14,28}

Nevertheless, despite the above-mentioned complications, we will compare our results with those of *c*-Si. Therefore, in Fig. 3, we compare the squared linear susceptibility $|\chi^{(1)}|^2$ of *c*-Si with the $|\chi^{(1)}|^2$ of the 9 nm thick *a*-Si:H film obtained by spectroscopic ellipsometry measurements. Note, that for *a*-Si:H, only one broad peak is observed due to the disorder in the amorphous film. The resonance that shows up in the SHG signal for *c*-Si at a photon energy of ~ 1.65 eV (SHG photon energy ~ 3.3 eV) is generally very pronounced for the oxidized surface.^{15,16} Based upon its similarities with the peak at 3.4 eV, as observed in the $|\chi^{(1)}|^2$ of *c*-Si, the resonance in the SHG signal for *c*-Si at a fundamental photon energy of ~ 1.65 eV has been attributed to a two-photon transition from Si-Si bonds in a strained surface layer.¹⁵ A similar contribution to the SHG signal might also be expected for the O₂-dosed *a*-Si:H film, although the disorder in the amorphous film might lead to a broader resonance characteristic. In Fig. 2 [most clearly in (a) and (c)], a broad feature is observed with a maximum SHG intensity around a two-photon energy of ~ 3.3 eV. The agreement between $|\chi^{(1)}|^2$ and the SHG signal after O₂ dosing suggests that the SHG signal is due to surface Si-Si bonds in a two-photon direct interband transition.

For the as-deposited film, however, especially the (*p*, *P*) and (*mix*, *S*), the SHG signals change significantly when subjected to the O₂ dosing (see Fig. 2). Although not abundant ($< 10^{12}$ cm⁻²) on the H-passivated *a*-Si:H surface, surface dangling bonds form a plausible explanation for these changes in the SHG signal, since O₂ quenches dangling bond defect states very efficiently, as was shown for *c*-Si surfaces.^{14,15,25} The dangling bond defect states form a continuous distribution of localized states in the band gap of *a*-Si:H, which can be expected to result in a spectrally broad SHG signal, particularly apparent below photon energies of 1.3 eV and similar to the *c*-Si case. This would also be in line with the aforementioned fact that dangling bonds in the bulk and surface region of *a*-Si:H are probed in this photon energy range by subgap absorption spectroscopy.^{19,20} On the

basis of this reasoning, the effect observed for the (*p*, *P*) polarization configuration appears to be straightforward: when the film is exposed to O₂, the signal below 1.3 eV drops due to the quenching of the dangling bond surface states and only the Si-Si direct interband transition remains. Here, we make the implicit assumption that the signal due to Si-Si bonds is also observed for the as-deposited *a*-Si:H film, which is not unreasonable as a SHG signal due to surface Si-Si bonds has also been observed for unreconstructed and H-terminated *c*-Si surfaces.^{11,14} However, the situation is very complicated for the (*p*, *P*) polarization configuration as this signal depends on all three independent components of the second-order susceptibility tensor. On the other hand, the (*mix*, *S*) SHG signal depends only on one tensor component $\chi_{xyz}^{(2)}$ and interpretation of the SHG signal should be easier. Nevertheless, it seems unlikely that this tensor component is almost zero for an isotropic surface prior to O₂ dosing as can be seen in Fig. 2(c). A possible explanation for this observation is destructive interference between different contributions to the SHG signal that have significant spectral overlap, such as, e.g., the interband transition due to Si-Si bonds and the resonance due to dangling bonds. If these dangling bond surface states are quenched by O₂, the destructive interference disappears and the broad SHG resonance of the Si-Si direct interband transition is revealed (see Fig. 2). Finally, considering the (*s*, *P*) polarization configuration, it appears the SHG signal remains virtually unchanged. Yet, real-time SHG measurements at a photon energy of 1.2 eV during O₂ dosing of the 9 nm thick *a*-Si:H film (not shown) have revealed an initial fast decrease in SHG signal almost down to zero followed by a slow recovery of the signal to about half its initial value before O₂ dosing (in agreement with Fig. 2). This can possibly be explained by a rapid quenching of the dangling bond surface states, while incorporation of oxygen in the surface layer largely restores the SHG signal due to the broad resonance of the surface Si-Si direct interband transition at 3.3 eV.

From these considerations, it is clear that it is very complicated to determine the microscopic origin of the SHG signal generated by the *a*-Si:H surface and more experimental investigations are required to be more conclusive. However, it shows also that it is a plausible working hypothesis for the moment to assume the SHG signal of *a*-Si:H is generated primarily by surface dangling bonds for photon energies below 1.3 eV and by surface Si-Si bonds in a direct interband transition for higher photon energies.

The hypothesis can be further verified by a simple model of the frequency dependent nonlinear response of the *a*-Si:H thin film (the spectra as presented in Fig. 2) using a coherent superposition of only two resonances, i.e., of the dangling bonds and of the Si-Si bonds, with excitonic line shapes as an *ansatz*^{14,21,28-30}

$$\chi^{(2)}(2\omega) = \sum_{n,m} \left\{ \frac{f_n \exp(i\varphi_n)}{\omega - \omega_n + i\gamma_n} + \frac{f_m \exp(i\varphi_m)}{2\omega - \omega_m + i\gamma_m} \right\}. \quad (2)$$

We assume the resonance frequencies ω_n and ω_m centered at 1.1 and 1.65 eV for the dangling bond and the Si-Si direct interband transitions, respectively. The damping constants γ ,

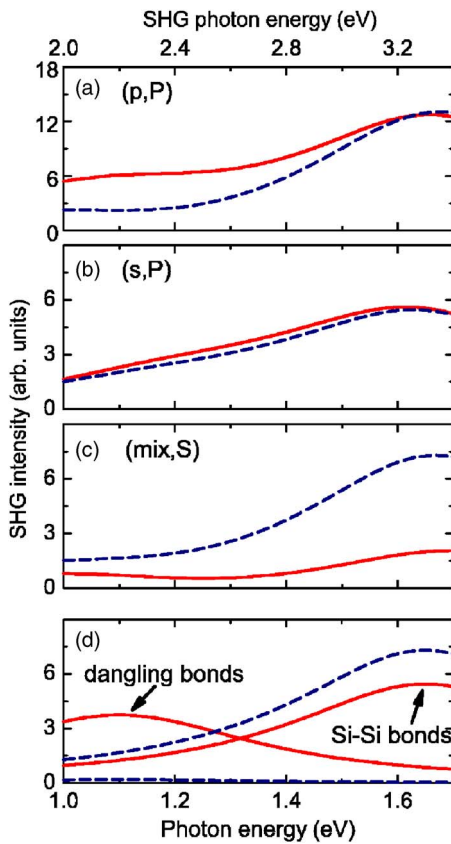


FIG. 4. (Color online) Simulated SHG spectra for the three polarization combinations (a) (p,P) , (b) (s,P) , and (c) (mix,S) to reproduce the measured SHG spectra shown in Fig. 2. Solid and dashed lines refer to the as-deposited and O_2 dosed cases, respectively. In (d), the two resonances used in the simulations to generate the (mix,S) spectra are shown as an example.

representing the linewidth of the resonance, are assumed 0.3 eV for both resonances. These values for the resonance frequencies and the linewidths are based on the optical linear properties of a -Si:H,^{18–20} while the amplitude f and phase φ of the resonances are modeling parameters. The simulated spectra, qualitatively reproducing the measured spectra in Fig. 2 to a fair extent, are shown in Fig. 4. It is clear that the almost zero SHG signal for (mix,S) for the as-deposited film can be reproduced by imposing destructive interference between the two resonances that are shown in Fig. 4(d) as an example (solid lines). Furthermore, when quenching the amplitude of the dangling bond resonance as a result from O_2 dosing, the measured SHG spectrum in Fig. 2(c) is obtained showing only the signal due to Si-Si bonds [with only a small change in the amplitude of the Si-Si direct interband resonance, dashed line in Fig. 4(c)]. For (s,P) and (p,P) , a similar good agreement has been obtained by optimization of the independent modeling parameters.³¹ Only the dip in the measured spectra at 1.3 eV could not be reproduced in the simulated spectra which can be related to the small transmission of the optical system at this energy or due to the oversimplified model. In any case, it can be concluded that the model gives further support for the presented interpretation of the SHG signal.

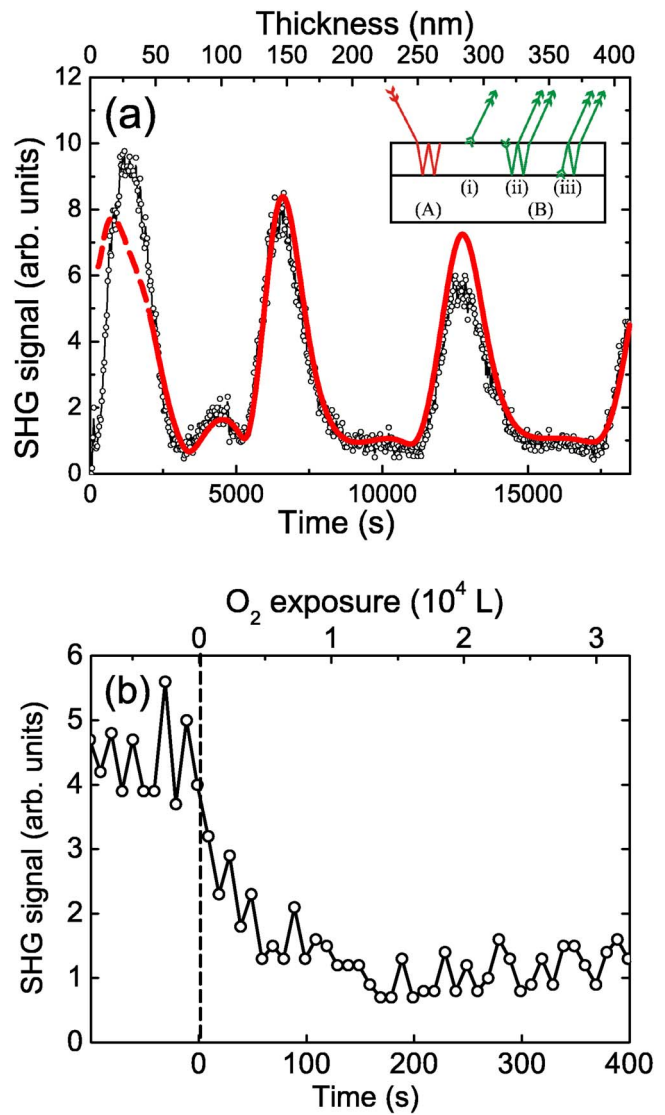


FIG. 5. (Color online) Real-time SHG signal as measured (a) during a -Si:H deposition (30 s intervals between data points) and (b) during exposure of the 412 nm thick a -Si:H film to O_2 (10 s intervals between data points). The solid line in (a) is a fit to the SHG data using a model that takes into account interference effects of the fundamental (A) and SHG radiation (B) in the thin film as well as the SHG radiation produced at the surface (i)+(ii) and at the buried interface (iii) (see inset). The fit is optimized for a film thickness > 50 nm. In (b), the as-deposited film is exposed to O_2 starting at $t=0$ s.

The potential of the SHG technique to detect surface states can be further illustrated by real-time measurements during film growth. Here, we show the first real-time SHG observation during the growth of an a -Si:H film starting from a clean fused silica substrate up to a ~ 412 nm final film thickness for a photon energy of 1.2 eV. The (p,P) polarization configuration was chosen as it yielded the largest signal. The SHG signal in Fig. 5(a) shows very strong thickness dependence that can be explained by interference of both the fundamental radiation (A) and the SHG radiation (B) in the thin film, and interference between the three separate contributions to the total SHG signal: (i) the *reflected*

SHG contribution from the surface, (ii) the *transmitted* SHG contribution from the surface into the film that is reflected back from the buried interface, and (iii) the *reflected* SHG contribution from the buried interface [see inset Fig. 5(a)]. With increasing thickness, the contributions (ii) and (iii) will diminish due to strong absorption of the SHG radiation in the film, and finally disappear when the film, at a film thickness of approximately 150 nm, becomes opaque for the SHG radiation. This is reflected in Fig. 5(a): above a thickness of 150 nm, the thickness dependence of the SHG signal shows a regular interference pattern that can simply be explained by interference of the fundamental radiation (A) in the film as there is only a contribution from (i); below 150 nm, however, a deviation from this regular interference pattern is observed (e.g., the local maximum at ~ 90 nm) which can only be explained by considering all three SHG contributions (i)–(iii) as well as taking into account both the interference of the fundamental radiation (A) and the SHG radiation (B) in the film. Using the theory developed by Sipe *et al.*³² and taking into account the above-mentioned contributions, the thickness dependence could be fitted in a straightforward way^{30,33} as shown by the solid line in Fig. 5(a). We find good agreement except for the first 50 nm in which deviation from the actual data is observed. This deviation can probably be explained by the fact that during the initial growth stage, the microstructural (e.g., surface roughness) and optical properties of the thin film change considerably as revealed by spectroscopic ellipsometry.^{34,35}

Consequently, by using a sufficiently thick film (>150 nm), the SHG signal generated from the surface can be isolated from the SHG signal generated at the buried interface. This makes it possible to explicitly prove the SHG signal originates from surface (defect) states by exposing the film to O_2 . Film growth was, therefore, terminated at a maxi-

mum in the SHG signal [see Fig. 5(a)] in order to obtain the best sensitivity. Immediately after termination of film growth, the reactor chamber was backfilled with O_2 at a pressure of 7.5×10^{-5} Torr while recording the SHG signal. Figure 5(b) shows the SHG signal decreases as a function of exposure until only a relatively small signal remains. This remaining SHG signal can be due to the (non-) resonant surface and bulk contributions to the SHG signal as mentioned earlier. This experiment clearly demonstrates the SHG signal at this photon energy is sensitive to surface states of the a -Si:H film.

IV. CONCLUSIONS

The SHG response of as-deposited a -Si:H thin films was investigated *in situ* with respect to polarization and spectral dependence. Dosing the film with O_2 showed the SHG radiation has a contribution from the isotropic a -Si:H surface. On the basis of a comparison with c -Si, the microscopic origin of the SHG signal is discussed and it is made plausible that it originates from direct interband transition due to Si-Si bonds and dangling bond surface states. Finally, the first SHG experiment during real-time a -Si:H growth is presented showing the potential of the technique for monitoring surface (defect) states of a -Si:H.

ACKNOWLEDGMENTS

This work has been supported by the Netherlands Foundation for Fundamental Research on Matter (FOM) and the research of W. K. has been made possible by a fellowship of the Royal Netherlands Academy of Arts and Sciences (KNAW). The skillful technical assistance of M. J. F. van de Sande, J. F. C. Jansen, A. B. M. Hüsken, and H. M. M. de Jong is acknowledged.

*Corresponding author. Email address: w.m.m.kessels@tue.nl

¹A. Gallagher, Mater. Res. Soc. Symp. Proc. **70**, 3 (1986).

²A. Matsuda and K. Tanaka, J. Appl. Phys. **60**, 2351 (1986).

³A. Matsuda, K. Nomoto, Y. Takeuchi, A. Suzuki, A. Yuuki, and J. Perrin, Surf. Sci. **227**, 50 (1990).

⁴M. S. Valipa, E. S. Aydil, and D. Maroudas, Surf. Sci. Lett. **572**, L339 (2004).

⁵A. Von Keudell and J. R. Abelson, Phys. Rev. B **59**, 5791 (1999).

⁶S. Yamasaki, T. Umeda, J. Isoya, and K. Tanaka, Appl. Phys. Lett. **70**, 1137 (1997).

⁷U. K. Das, T. Yasuda, and S. Yamasaki, Phys. Rev. Lett. **85**, 2324 (2000).

⁸M. Jeong, B. Doris, J. Kedzierski, K. Rim, and M. Yang, Science **306**, 2057 (2004).

⁹W. M. M. Kessels, J. J. H. Gielis, I. M. P. Aarts, C. M. Leewis, and M. C. M. van de Sanden, Appl. Phys. Lett. **85**, 4049 (2004).

¹⁰T. F. Heinz, in *Nonlinear Surface Electromagnetic Phenomena*, edited by H. Ponath and G. Stegeman (Elsevier, Amsterdam, 1991), p. 353.

¹¹U. Höfer, Appl. Phys. A **63**, 533 (1995).

¹²K. Pedersen and P. Morgen, Phys. Rev. B **52**, R2277 (1995).

¹³K. Pedersen and P. Morgen, Surf. Sci. **377-379**, 393 (1997).

¹⁴T. Suzuki, Phys. Rev. B **61**, R5117 (2000).

¹⁵W. Daum, H. J. Krause, U. Reichel, and H. Ibach, Phys. Rev. Lett. **71**, 1234 (1993).

¹⁶Y. Q. An and S. T. Cundiff, Appl. Phys. Lett. **81**, 5174 (2002).

¹⁷P. Lautenschlager, M. Garriga, L. Vina, and M. Cardona, Phys. Rev. B **36**, 4821 (1987).

¹⁸R. A. Street, *Hydrogenated Amorphous Silicon* (Cambridge University Press, Cambridge, 1991).

¹⁹A. Asano and M. Stutzmann, J. Appl. Phys. **70**, 5025 (1991).

²⁰I. M. P. Aarts, B. Hoex, A. H. M. Smets, R. Engeln, W. M. M. Kessels, and M. C. M. van de Sanden, Appl. Phys. Lett. **84**, 3079 (2004).

²¹G. Erley and W. Daum, Phys. Rev. B **58**, R1734 (1998).

²²S. Alexandrova, P. Danesh, and I. A. Maslyanitsyn, Phys. Rev. B **61**, 11136 (2000).

²³S. Alexandrova, P. Danesh, and I. A. Maslyanitsyn, Vacuum **69**, 391 (2003).

²⁴ P polarization with respect to the SHG experimental setup which corresponds to S polarization with respect to the monochromator's grating.

- ²⁵P. Bratu, K. L. Kompa, and U. Höfer, Phys. Rev. B **49**, R14070 (1994).
- ²⁶N. Blayo and B. Drévillon, Surf. Sci. **260**, 37 (1991).
- ²⁷J. I. Dadap, B. Doris, Q. Deng, M. C. Downer, J. K. Lowell, and A. C. Diebold, Appl. Phys. Lett. **64**, 2139 (1994).
- ²⁸K. Pedersen and P. Morgen, Phys. Status Solidi C **0**, 3065 (2003).
- ²⁹G. Erley, R. Butz, and W. Daum, Phys. Rev. B **59**, 2915 (1999).
- ³⁰J. J. H. Gielis, I. M. P. Aarts, M. C. M. Van de Sanden, and W. M. M. Kessels (unpublished).
- ³¹The (mix, S) and (s, P) SHG signals are determined by single, independent nonlinear tensor components and can, therefore, be simulated separately; whereas, for the (p, P) polarization case, the amplitude and phase information as obtained from the simulations of the (mix, S) and (s, P) configurations have to be taken into account because the (p, P) SHG signal depends on all three independent nonlinear tensor components simultaneously.
- ³²J. E. Sipe, D. J. Moss, and H. M. van Driel, Phys. Rev. B **35**, 1129 (1987).
- ³³B. Koopmans, A. Anema, H. T. Jonkman, G. A. Sawatzky, and F. Van der Woude, Phys. Rev. B **48**, 2759 (1993).
- ³⁴I. An, H. V. Nguyen, N. V. Nguyen, and R. W. Collins, Phys. Rev. Lett. **65**, 2274 (1990).
- ³⁵W. M. M. Kessels, J. P. M. Hoefnagels, E. Langereis, and M. C. M. Van de Sanden, Thin Solid Films (to be published).